

STUDENT SUMMER INTERNSHIP TECHNICAL REPORT

Iodate Reduction and Dissolution by Dithionite of Hanford Sediments

DOE-FIU SCIENCE & TECHNOLOGY WORKFORCE DEVELOPMENT PROGRAM

Date submitted:

September 14, 2018

Principal Investigators:

Silvina Di Pietro (DOE Fellow Student)
Hilary P. Emerson, Ph.D., EIT (Research Scientist)
Florida International University

Jim Szecsody, Ph.D., P.G. 1497 (Mentor)
Pacific Northwest National Laboratory

Florida International University Program Director:

Leonel Lagos Ph.D., PMP®

Submitted to:

U.S. Department of Energy
Office of Environmental Management
Under Cooperative Agreement # DE-EM0000598



Applied Research Center
FLORIDA INTERNATIONAL UNIVERSITY

DISCLAIMER

This report was prepared as an account of work sponsored by an agency of the United States government. Neither the United States government nor any agency thereof, nor any of their employees, nor any of its contractors, subcontractors, nor their employees makes any warranty, express or implied, or assumes any legal liability or responsibility for the accuracy, completeness, or usefulness of any information, apparatus, product, or process disclosed, or represents that its use would not infringe upon privately owned rights. Reference herein to any specific commercial product, process, or service by trade name, trademark, manufacturer, or otherwise does not necessarily constitute or imply its endorsement, recommendation, or favoring by the United States government or any other agency thereof. The views and opinions of authors expressed herein do not necessarily state or reflect those of the United States government or any agency thereof.

ABSTRACT

DOE Fellow, Silvina A. Di Pietro, completed a 10-week internship with Pacific Northwest National Laboratory (PNNL) in Richland, Washington State. The objective of the study was to investigate a strategy for treatment of contaminated sediments with dithionite to release iodine. Under the mentorship of Dr. Jim Szecsody, she conducted a series of batch experiments understanding (1) the influence of variable solution components on iodine leaching from contaminated sediments, and (2) the rate of iodine removal by sodium-dithionite solutions. Dithionite was used in these experiments as it can both reduce iodate to iodide and dissolve iron oxides on sediment surfaces. Samples varied in reaction time, initial iodate concentration, sodium-dithionite treatment concentration, and sediments as they were recovered from variable depths and locations at the Hanford site. In addition, PhD candidate Di Pietro received invaluable guidance in experimental design and development that will benefit her ongoing research endeavors.

TABLE OF CONTENTS

ABSTRACT.....	iii
TABLE OF CONTENTS.....	iv
LIST OF FIGURES	v
LIST OF TABLES	vi
1. INTRODUCTION	1
2. EXECUTIVE SUMMARY	5
3. MATERIALS AND METHODS.....	6
4. RESULTS AND ANALYSIS.....	10
5. CONCLUSION.....	15
6. REFERENCES	16
APPENDIX A.....	17

LIST OF FIGURES

Figure 1. Plume map of ^{129}I contamination in the Hanford 200 Area (Lee et al., 2017).....	2
Figure 2. Pourbaix diagram of aqueous iodine speciation; solid line = total iodine concentration of 1 $\mu\text{g/L}$, a typical groundwater concentration, dotted line = total iodine concentration of 3	3
Figure 3. Conceptual overview of subsurface biogeochemical processes that affect the fate and transport of iodine. Note: the diagram does not distinguish between ^{129}I and ^{127}I because these processes are the same for both isotopes (Truex et al., 2017)	4
Figure 4. Set-up for sampling day #1 (1 h) of long-term stability of iodine leaching batch experiment.....	9
Figure 5. ^{127}I extracted from sediment C9510 114.3-115.3' for samples E80-83 with variable carbonate: 0.1 M Na- dithionite (light orange), 0.1 M Na- dithionite+ 0.4 M K_2CO_3 (mid-orange), 1 M Na-dithionite + 0.4 M K_2CO_3 + 0.4 M Na-citrate (orange) for seven-day contact time and 1 M Na-dithionite + 0.4 M K_2CO_3 changing solution every 48 hours (dark orange)....	10
Figure 6. Iodine-127 extracted from soil sediments sample E84 - borehole C9507 104.4-105.4' (blue), sample E85 - borehole C9510 114.3.115.3' (red), and sample E86 borehole - C9507 94.1-95.1' by 1 M Na-dithionite + 0.4 M K_2CO_3 in artificial groundwater solution as a function of time expressed in log hours.....	12
Figure 7. Pseudo second-order kinetics fit for iodate-contaminated ($\sim 100 \mu\text{g/L}$) Hanford Site sediments; sample E84 (blue), sample E85 (red), and sample E86 (green).	13
Figure 8. Reaction order plot of natural logarithm for the pseudo second-order rate using Eq. 5 against the natural logarithm of iodide concentration (in $\mu\text{g/L}$) for iodate-contaminated ($\sim 100 \mu\text{g/L}$) Hanford Site sediments; sample E84 (blue), sample E85 (red), and sample E86 (green)..	13
Figure 9. National Historic Landmark Nuclear Production Plant B-reactor constructed in 1943-1944.....	17
Figure 10. DOE Silvina Fellow Di Pietro in front of the B-Reactor National Historic Landmark entrance.	18
Figure 11. Nuclear Magnetic Resonance (NMR) coupled with Ion Cyclotron Resonance (ICR) instrument with 21.1 Tesla fields (900 MHz 1H frequency) from EMSL facility.	18
Figure 12. 3-D printing facility showing batteries and spherical balls Matryoshka-design as samples.....	19
Figure 13. Tanks in the Aquatic Research Laboratory; guided tour by P.I. Timothy Linley.	19
Figure 14. Jonathan Williams, MSIPP fellow and FIU biomedical engineering student, with DOE Fellow Silvina Di Pietro in front of one of the two detector arms of the Laser Interferometer Gravitational-Wave Observatory (LIGO) at Hanford, WA.	20
Figure 15. FF-5 Stage B polyphosphate tanks in the 300 Area treatment field.....	20
Figure 16. One of the 48 wells (painted yellow) dug into the subsurface of the FF-5 Stage B, 300 Area treatment field (Columbia River pictured at the right).....	21
Figure 17. Contractors (right) show PNNL scientists (left) how the pump delivers the polyphosphate solution to the wells.....	21

LIST OF TABLES

Table 1. Major sources of ^{129}I in the environment (Truex et al., 2017).....	2
Table 2. Artificial Groundwater Composition used for Iodine Batch Experiments	6
Table 3. Part A batch experiment data, including samples, solution volume and concentration, sediment mass, and starting and elapsed time, to evaluate variable carbonate concentrations	7
Table 4. Summary of rate laws, integrated rate law linear equations and plots variables for different kinetic models	8
Table 5. Part C batch experiment of long-term stability of iodine leaching parameters. Note: volume and reductant solution were the same as Part B	9
Table 6. Kinetic parameters (rate law, standard deviation taken from linear regression, R^2 values and half-life) for zero-order, first-order and pseudo second-order models for the iodine released into the 1 M Na-dithionite + 0.4 M K_2CO_3 solution in samples E84-86	12

1. INTRODUCTION

Radioactive isotopes of iodine are produced from neutron-induced fission of uranium (U) and plutonium (Pu) in nuclear reactors. However, they can also be produced naturally in small quantities from spontaneous fission of natural U. Nuclear reactions can form up to 19 iodine isotopes from fission products (Kantelo, Bauer, Marter, Murphy Jr, & Zeigler, 1993). However, only ^{129}I isotope is of long-term concern with a half-life of 16 million years (Kaplan et al., 2014).

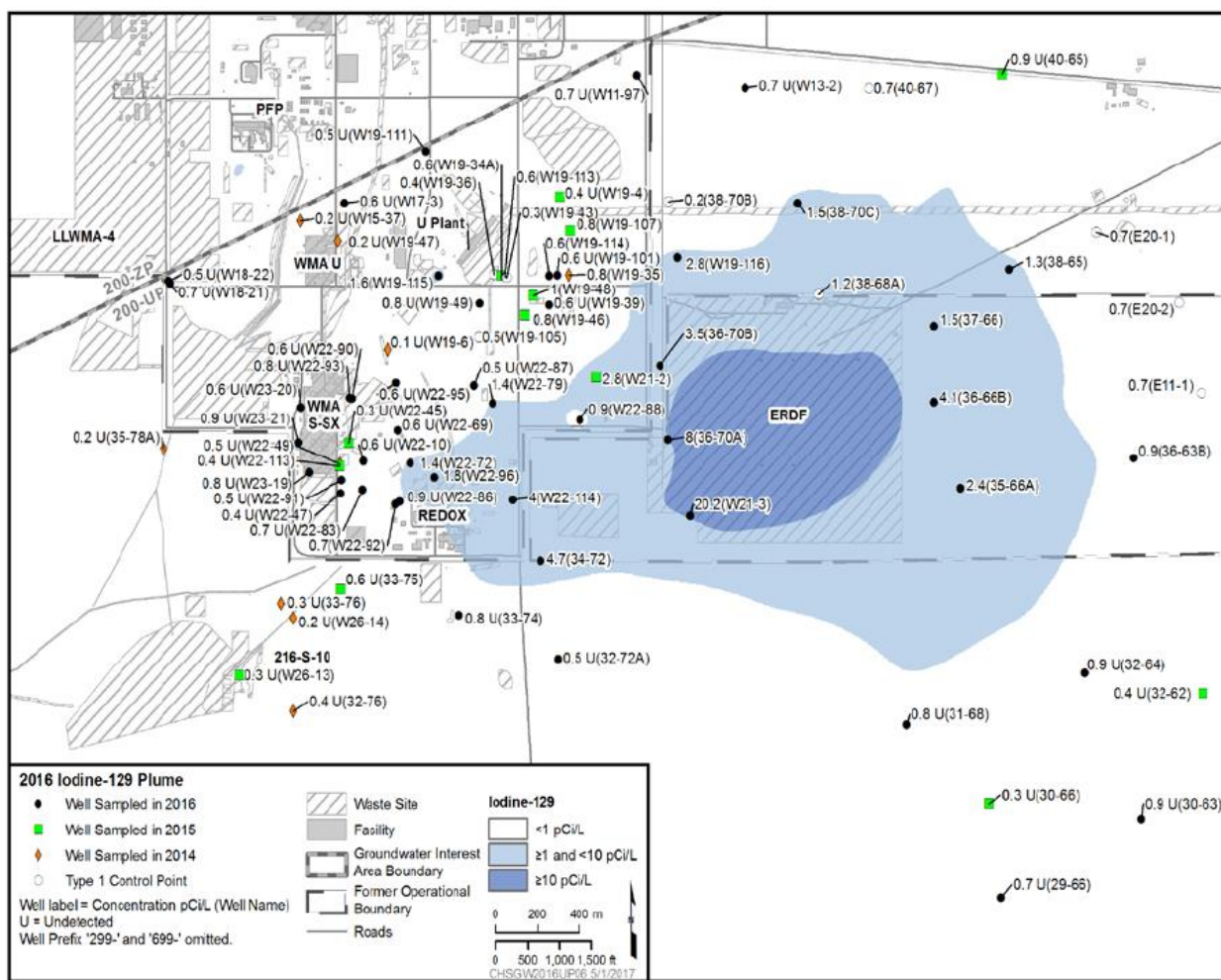
Iodine-129 (^{129}I) generated at the U.S. Department of Energy (DOE) Hanford Site during Pu production was released to the subsurface resulting in several large, dilute plumes in the groundwater. As depicted in Table 1, the Hanford Site is one of the major contributors to worldwide release of ^{129}I to the environment. Currently, the 200 West Area of the Hanford Site holds the majority of the ^{129}I groundwater contamination with three plumes covering an area $> 50 \text{ km}^2$ (Kaplan et al., 2014). In 2016, Lee and his research team sampled and analyzed the 200 Area wells for both ^{127}I and ^{129}I for the area shown in Figure 1. The total ^{129}I within the wells was very small ($10^{-3} - 10^{-5} \text{ } \mu\text{g/L}$) (Szecsody et al., 2017). However, despite its low concentration, ^{129}I dilute plumes exceed the minimum Federal Register drinking water standard of 1.0 pCi/L (Kaplan et al., 2014).

For environmental iodine chemistry, three iodine species are of concern: iodide (I_2), iodide (I^-) and iodate (IO_3^-). As the Pourbaix diagram shows in Figure 2, I^- and IO_3^- are the most stable species. Although I^- covers a significant range of Eh-pH conditions and appears to be close to the limits of water (dashed lines), IO_3^- is the major species present at the Hanford Site. Organo-iodine can also be significant but has not been characterized for inclusion in Pourbaix diagrams. Groundwater analysis reported that 85% of the total aqueous iodine mass was IO_3^- (Szecsody et al., 2017), however iodine extraction from vadose zone sediments indicates most sediments have more iodide than iodate mass. Although the vadose zone and unconfined aquifer is oxic to suboxic, there are abiotic reductants in the mafic sediments and iodate microbial reduction can also occur.

Reported K_d values on Hanford Site sediments show a very low sorption of iodide ($< 0.23 \text{ mL/g}$) and about four times greater sorption for iodate (Truex et al., 2016). However, 80-97% of the iodine is still bound in the solid phase at the Hanford site. Iodate and organo-iodine are generally more retarded than I^- because of their strong interaction with clays and organic matter. The initial intent of dithionite addition (as a part of a pump and treat system) is to reduce adsorbed iodate to Iodide to more quickly advect iodine mass out of the aquifer. However, dithionite treatment of sediment also dissolves and reduces Fe(III) oxides (Szecsody et al., 2004), so additional Fe-oxide-bound iodine mass is also removed from the sediment. Sequential extractions of iodine-contaminated sediments have shown that 80 to 97% of the iodine is in solid phases (Truex et al., 2017, Szecsody et al., 2017). It has been hypothesized that this includes Fe oxides and calcite. The focus of this study is on the use of a dithionite solution to extract iodine from contaminated sediments by: a) reduction of adsorbed iodate, and b) dissolution of Fe(III) oxides that contain iodine (likely iodate).

Table 1. Major sources of ^{129}I in the environment (Truex et al., 2017)

Source	^{129}I Mass Released (kg)	Reference
Fuel reprocessing at La Hague (France)	3800	Hou <i>et al.</i> 2009
Fuel reprocessing Sellafield (UK)	1400	Hou <i>et al.</i> 2009
Hanford Site	266	Raisbeck and Yiou 1999
Natural hydrosphere and atmosphere	100	Bustad <i>et al.</i> 1983
Atmospheric weapons testing	50	Raisbeck and Yiou 1999
Savannah River Site	32	Kantelo <i>et al.</i> 1990
Nevada Test Site Underground nuclear testing	10	Raisbeck and Yiou 1999
Chernobyl	1-2	Raisbeck and Yiou 1999
Fukushima	1.2	Hou <i>et al.</i> 2013

**Figure 1. Plume map of ^{129}I contamination in the Hanford 200 Area (Lee et al., 2017)**

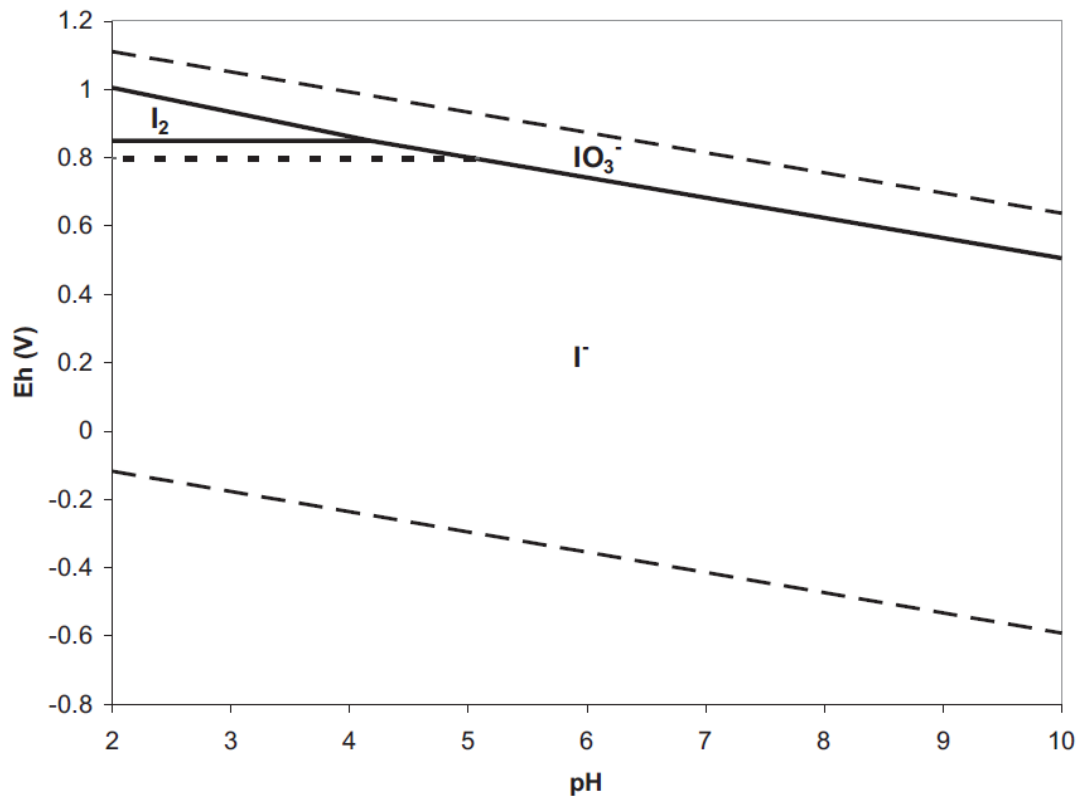


Figure 2. Pourbaix diagram of aqueous iodine speciation; solid line = total iodine concentration of 1 $\mu\text{g/L}$, a typical groundwater concentration, dotted line = total iodine concentration of 58 $\mu\text{g/L}$, a typical seawater concentration; dashed lines = stability limits of water (Fuge et al., 1986; Kaplan et al., 2014)

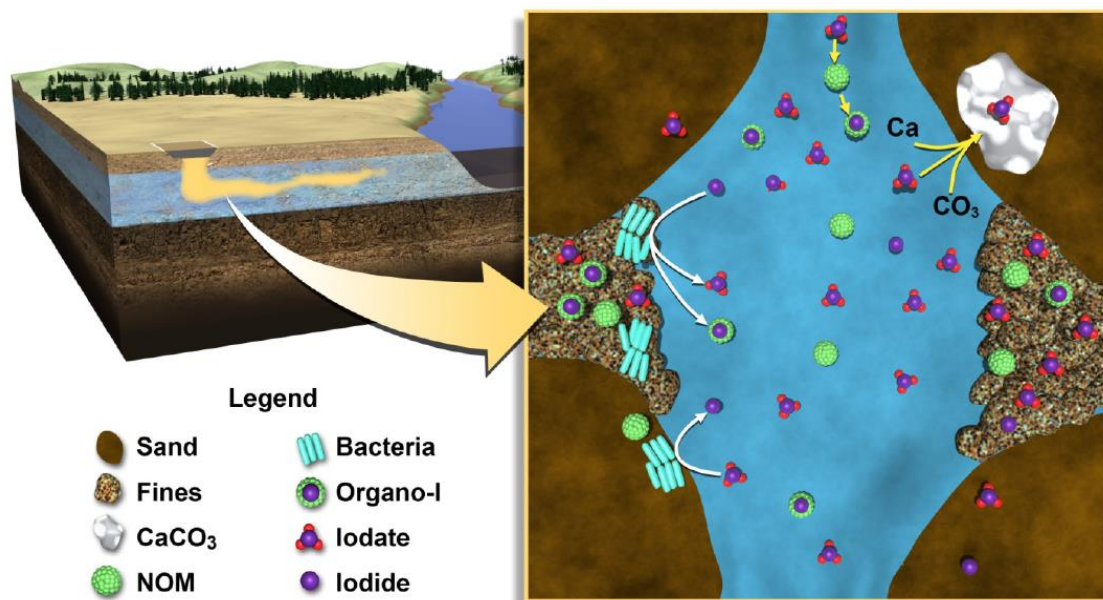


Figure 3. Conceptual overview of subsurface biogeochemical processes that affect the fate and transport of iodine. Note: the diagram does not distinguish between ^{129}I and ^{127}I because these processes are the same for both isotopes (Truex et al., 2017)

In previous research, scientists found that reduction of various contaminants was fast in the presence of strong reductants, such as zero-valent iron and sulfur-modified iron (Devlin & Müller, 1999; Szecsody et al., 2004; Waybrant, Blowes, & Ptacek, 1998). Iodate reduction can occur, as Hanford vadose zone sediments showed that the iodate reduction rate that varied two orders of magnitude from 0.06 to 23 pmol/h/g with no treatment (Szecsody et al., 2017). In one study, dithionite-reduction of Fe oxides in sediment had an average half-life of 6.5 hours (Szecsody et al., 2004). As we hypothesize that much of the iodine bound in solid phases in Hanford sediments is in Fe oxides, this Fe oxide dissolution rate may be similar to the release rate of iodine from sediment.

The objective of this internship was to develop an understanding of prior and ongoing research related to the treatment of the deep vadose zone using sodium-dithionite as a reductant to release iodine by working with PNNL scientists most familiar with the project. The report aims to contribute to our understanding of the fate and transport of the contaminant ^{129}I in contaminated Hanford Site sediments.

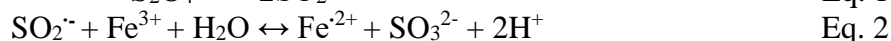
2. EXECUTIVE SUMMARY

This research work was supported by the DOE-FIU Science & Technology Workforce Initiative, an innovative program developed by the US Department of Energy's Office of Environmental Management (DOE-EM) and Florida International University's Applied Research Center (FIU-ARC). During the summer of 2018, DOE Fellow intern Silvina Di Pietro spent 10 weeks at a summer internship at Pacific Northwest National Laboratory (PNNL) in Richland, WA under the supervision and guidance of Dr. Jim Szecsody, a Senior Scientist with the Environmental Systems Group. The intern's project was initiated on June 4, 2018 and continued through August 10, 2018 with the objective of performing research and assisting with experiments related to the remediation of iodine-129 in the 200 Area of the Hanford Site in Washington State.

3. MATERIALS AND METHODS

The purpose of this research was to develop a technology to mobilize iodine under Hanford 200 Area groundwater conditions in order to remove radioactive iodine from the subsurface. These laboratory studies focused on identifying (1) variable carbonate concentrations and (2) the rate of iodine re-mobilization as sediments were exposed to dithionite ($\text{S}_2\text{O}_4^{2-}$) as a reductant. The goal was to release iodine from the solid phase by converting iodate (IO_3^-) to iodide (I^-) and by dissolving iron oxides on sediment surfaces.

Studies show that dithionite treatment reduces structural iron in clays by dissolving and reducing amorphous and some crystalline iron (III) oxides (Cervini-Silva, Larson, Wu, Stucki, & technology, 2001; Stucki, Golden, Roth, & Minerals, 1984). The rapid dissociation of the reductant anion (Eq. 1) allows for reduction of iron (III) solid phases given by Eq 2.



Batch experiments were conducted to quantify iodine dissolution into the aqueous phase. Experiments were aimed at understanding (1) the influence of variable components on iodine leaching from contaminated sediments (referred to as *Part A*) and (2) the rate of iodine re-mobilization by sodium-dithionite solution (referred to as *Part B*). Finally, *Part C* or the long-term stability of iodine leaching batch experiment is an extension of *Part B*, where the three contaminated sediments (E84-86) from *Part B* were sampled at longer times. Experiments used artificial groundwater (Table 2), ambient temperature (20-22°C), aquifer sediments with a pH of 7.7-8.3, and field iodine-contaminated ($\sim 100 \mu\text{g/L}$) and uncontaminated sediments from operable unit (OU) 200-UP-1 (Figure 1). Aqueous iodine analysis was performed in the Energy Systems Laboratory (EML) located in Building 331 of the Subsurface Science and Technology Group using an ion-chromatograph (operating procedure OP-DVZ-AFRI-001) coupled with an inductively coupled plasma mass spectrometer (ICP-MS).

Table 2. Artificial Groundwater Composition used for Iodine Batch Experiments

Constituent	Concentration (mg/L)	Molarity (mmol/L)
$\text{H}_2\text{SiO}_3 \cdot n\text{H}_2\text{O}$, silicic acid	15.3	0.154
KCl, potassium chloride	8.20	0.110
MgCO_3 , magnesium carbonate	13.0	0.154
NaCl, sodium chloride	15.0	0.257
CaSO_4 , calcium sulfate	67.0	0.492
CaCO_3 , calcium carbonate	150	1.50

Part A. Influence of Variable Components on Iodine Leaching from Contaminated Sediments

An experiment was conducted on contaminated ($\sim 100 \mu\text{g/L}$) ^{127}I -oxidized from Hanford Site sediment from borehole C9510 114.3-115.3'. Batch experiments consisted of four 45 mL polycarbonate centrifuge tubes in which $\sim 5.0 \text{ g}$ of sediment was reacted with 20 mL of reductant solution (253 g/L). The solution was prepared as follows: 0.4325 g of Na-dithionite in 250 mL of artificial groundwater (Table 2) for sample ID E80; 0.4325 g of Na-dithionite and 1.382 g of K_2CO_3 in 250 mL of artificial groundwater for sample ID E81; and the same protocol for sample ID E82, with the exception of adding 0.100 g of KHCO_3 . The carbonate buffer is necessary as four moles of H^+ are produced per mole of dithionite consumed, as described in Eq. 2 (Szecsody et al., 2004). The order of the reagents is important as the presence of dithionite in aqueous solution will disproportionate (Eq. 1) at a rate of ~ 5 minutes, resulting in unavailability for iron reduction (Zachara et al., 2000)(Zachara et al., 2000). A carbonate buffer (K_2CO_3) was added first, followed by KHCO_3 . Nitrogen gas was bubbled for ~ 30 minutes to remove dissolved oxygen. Lastly, Na-dithionite was added inside the anaerobic chamber (Coy Laboratory). Samples E80-82 were sampled after seven days of contact time. With a 10 mL syringe needle, 2.0 mL of sample was removed and filtered through a $0.45 \mu\text{m}$ filter. Samples were placed in 5 mL plastic vials for analysis. Analysis of iodine species was conducted using an ion-chromatograph (operating procedure OP-DVZ-AFRI-001) coupled with a mass analyzer (ICP-MS) from PNNL's Energy Systems Laboratory (EML). It is important to note that sample ID E83 was sampled every 48 hours by removing the 0.4 M K_2CO_3 + 0.1 M Na-dithionite solution and adding a fresh volume (20 mL) of the same solution (for a total of three times). The purpose of adding fresh solution was to determine if higher iodine concentrations would be extracted in comparison to the original, seven-day contact solution. Table 3 below lists the solution concentrations for all four samples in accordance with their sampling times.

Table 3. Part A batch experiment data, including samples, solution volume and concentration, sediment mass, and starting and elapsed time, to evaluate variable solution components

Sample ID	Na-dithionite (mol/L)	K_2CO_3 (mol/L)	Na-citrate (mol/L)	Sediment (g)	Final solution (mL)	Start time (date, time)	End time (date, time)
E80	0.1	-	-	5.0675	20	6/11/18 14:53	6/18/2018 10:39
E81	0.1	0.4	-	5.1066	20	6/11/18 14:53	6/18/2018 10:44
E82	0.1	0.4	0.4	5.3282	20	6/11/18 14:53	6/18/2018 10:47
E83	0.1	0.4	-	5.1367	20	6/11/18 14:53	6/13, 6/15 and 6/18

Part B. Rate of Iodine Re-mobilization by Dithionite Solution

For Part B experiments, the sampling procedure and analyses were the same as Part A. Sampling times, however, ranged from 0.1 to 150 hours. In addition, the solid to liquid ratio was increased (from 253 to 288 g/L) to promote more iron oxide dissolution. It is important to note that the reductant solution was Na-dithionite with carbonate buffer, K_2CO_3 , (the same as E81 and E83 solutions) as previous studies show it to be the most promising treatment (Boparai, Comfort, Shea, & Szecsody, 2008; Szecsody et al., 2004; Zachara et al., 2000). Further, the kinetic release was used to describe Hanford sediment dissolution. The rate of reaction is often found to be proportional to the concentration of the reactants based to a power. For example, the rate of a change in concentration of a reactant (in this case "A" is Fe oxide concentration and "B" is the Na-dithionite concentration) to the molar concentration of two reactants A and B, written in Eq. 4 for the general reversible reaction in Eq. 3.



$$dA/dt = k_f[A]^a[B]^b \quad \text{Eq. 4}$$

The coefficient k_f is the forward rate coefficient for the reaction, dependent on the concentration of the species in the reaction (reactants A and B for Eq. 4). Further, sum of the powers to which the concentration of a species is raised is the order of the reaction (Atkins & DePaula, 2010). While Figure 7 below shows that the best fit for the rate laws follows a second order reaction, Figure 8 shows that this reaction order is occurring based on the slope of the line. A summary of different kinetic models can be found in Table 4.

Table 4. Summary of rate laws, integrated rate law linear equations and plots variables for different kinetic models

Kinetic Model	Rate Law	Linear Equation	Plot	Reference
Zero-order	$\frac{dC_t}{dC_o} = -k$	$[C_t] = [C_o] - kt$	$[C_t]$ vs. t	Atkins & DePaula, 2010
First-order	$\frac{dC_t}{dC_o} = -k[C_t]$	$C_t = C_o \cdot e^{-kt}$	$\ln [C_t]$ vs. t	Atkins & DePaula, 2010
Pseudo first-order	$\frac{dC_t}{dC_o} = -k[C_t]$	$C_t = C_o \cdot e^{-kt}$	$\ln([C_t]/[C_o])$ vs. t	Powell <i>et al.</i> , 2004 Abargues <i>et al.</i> , 2018
Second-order	$\frac{dC_t}{dC_o} = -k[C_t]^2$	$\frac{1}{C_t} = \frac{1}{C_o} + kt$	$1/C_t$ vs. t	Atkins & DePaula, 2010
Pseudo second-order	$\frac{dC_t}{dC_o} = -k[C_t]^2$	$\frac{1}{C_t} = \frac{1}{kC_o^2} + t \frac{1}{C_t}$	t/C_t vs. t	Gupta <i>et al.</i> , 2009

Part C. Long Term Stability of Iodine Leaching from Sediment - Batch System

For Part C experiments, the methodology was the same as Part B. This set of batch experiments, however, had two specific goals: (1) to understand the long-term stability of iodine leaching, thus the sampling times ranged from 0.1 to ~ 100s of hours, and (2) to understand the difference in iodine leaching between Na-dithionite-treated versus untreated sediments. Newly prepared 1 M Na-dithionite + 0.4 M K_2CO_3 solution was placed in both untreated sediments (samples E87, E89 and E91) and previously treated samples E84-86. To obtain the solid phase from Part B, samples E84-86 were centrifuged for 10 min at 3000 rpm (Sorvall Dupont RC5C). The supernatant was then discarded inside the fume hood (LabConco). This procedure was performed nine times for the following sampling periods: 1, 30, 90, 200, 300, 500, 750, 1000 and 1500 h. Figure 4 shows the experimental set-up for the long-term batch experiments as summarized in Table 5.

Table 5. Part C batch experiment of long-term stability of iodine leaching parameters. Note: volume and reductant solution were the same as Part B

Sample ID	Previous sample ID	Well	Mass (g)	Pre-treated with 0.1 M Na-dithionite + 0.4 M K_2CO_3
E87	-	C9507 104.4-105.4'	10.152	-
E88	E84	C9507 104.4-105.4'	10.048	☑
E89	-	C9510 114.3-115.3'	10.186	-
E90	E85	C9510 114.3-115.3'	10.092	☑
E91	-	C9507 94.1-95.1'	10.021	-
E92	E86	C9507 94.1-95.1'	10.069	☑

**Figure 4. Set-up for sampling day #1 (1 h) of long-term stability of iodine leaching batch experiment.**

4. RESULTS AND ANALYSIS

Part A. Influence of Variable Components on Iodine Leaching from Contaminated Sediments

Figure 5 shows the extracted iodide from Hanford site contaminated sediment C9510 under different solutions. Although the leaching amongst the different reductant solutions show a different yet increasing trend, sample E83 showed the most iodide ($59.8 \mu\text{mol/g}$) released after seven days of contact time. This is probably due to the frequent change in reductant liquid phase. The freshly added solution is not as oxidized as the one-time solution samples E80-82, and thus, solution sample E83 has a greater effect on reducing the iodine species found in the sediments. Every 48 hours, 20 mL of Na-dithionite and carbonate solution K_2CO_3 was added to sample E83 solid phase. When comparing E81 and E83 samples, there is an increase ($6.66 \mu\text{mol/g}$) in iodide leaching for the fresh dose of reductant solution (E83). This suggests that the 48 hour-change solution may have a slightly greater impact on contaminant mobility than the combination of three reductant solutions (citrate, carbonate buffer and Na-dithionite).

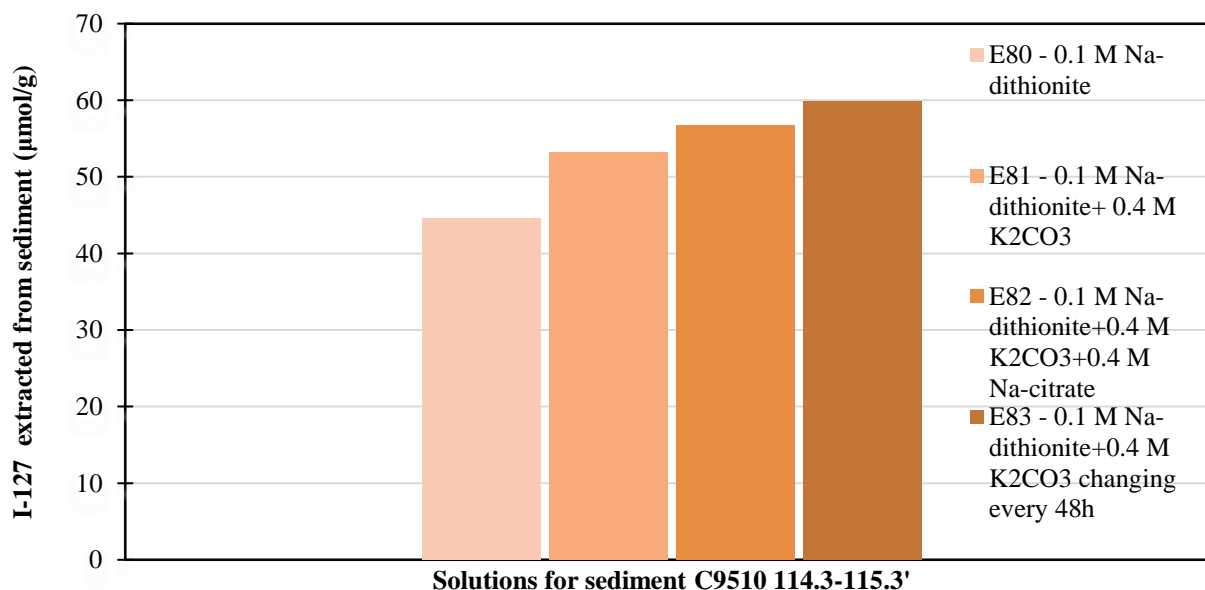


Figure 5. ^{127}I extracted from sediment C9510 114.3-115.3' for samples E80-83 with variable components: 0.1 M Na- dithionite (light orange), 0.1 M Na- dithionite+ 0.4 M K_2CO_3 (mid-orange), 1 M Na-dithionite + 0.4 M K_2CO_3 + 0.4 M Na-citrate (orange) for seven-day contact time and 1 M Na-dithionite + 0.4 M K_2CO_3 changing solution every 48 hours (dark orange).

Part B. Rate of Iodine Re-mobilization by Dithionite Solution

The goal for Part B experiments was to understand the dissolution of iron from Fe-oxides on Hanford Site sediments with respect to time. Upon ICP-MS analysis, the instrument's limit of detection (LOD) for iron was $1000 \mu\text{g/L}$. Due to its high LOD, all except for four sampling times from sample E86 gave an undetectable measurement. Instead, ^{127}I detectable measurements that were extracted from treated and untreated sediments were plotted as a function of time (in log hours) as shown in Figure 6. The iodide concentration extracted from the samples is $\text{E84} > \text{E85} > \text{E86}$. Iodide in sample E84 was over an order of magnitude (or 23 times larger) than sample E86.

For all three samples, there is no plateau reached in the 144 hours of contact time, suggesting further iodide leaching will occur over longer periods (i.e. steady state was not reached).

In addition, these data suggest that iodine is mobilized via a reduction mechanism as the dithionite is oxidized in solution. Qualitatively, dithionite removal was visually observed from the sediment color change from tan to gray (sample ID 84) or black (sample ID E85-86) as the contact time increased. This observation also indicates that the Fe-oxides particles on the Hanford Site sediments are reducing from ferric to ferrous iron.

In order to determine the coefficient k or rate laws for samples E84-86, the kinetic parameters shown in Table 4 were evaluated and plotted. Table 6 summarizes the determined parameters for iodine re-mobilized into the aqueous dithionite solution. When comparing the R^2 values for the different kinetic models, pseudo second-order has the best fit. Figure 7 below shows a plot of the linearized form of the pseudo-second order equation for iodine re-mobilized in the Hanford Site sediments. From Table 4, the correlation coefficients for the linear plot of t/C_t against time from the pseudo-second order rate law are greater than 0.984 for all three batch systems for contact times of up to 144 hours.

Furthermore, in order to be certain that a kinetic model follows a particular order, one can test the *method of initial rates* (Atkins & DePaula, 2010). This method plots the natural logarithm of the rate of the reaction against the natural logarithm of the concentration at a particular time, C_t . For samples E84-86, the latter (iodine concentration, C_t) was obtained from Figure 6. The former was obtained based on the general rate of reaction (Eq. 4 above). Assuming that the power is two (i.e., pseudo second-order reaction) and using the coefficient k or rate law from Table 6, the rate for samples E84-86 can be calculated. Eq. 5 below shows the reaction for the calculated rate.

$$\text{Rate} = k [I^-]^a \quad \text{Eq. 5}$$

where $a = 2$.

Upon plotting the calculated values and obtaining a linear equation, the slope is representative of the reaction order based on the method of initial rates. Figure 8 below shows the aforementioned plot with the natural logarithm of the calculated rate against natural logarithm of concentration C_t with a slope of an integer two. Both Figure 7 and Figure 8 conclude that the general reaction equation for this system (Eq. 2) follows a pseudo second-order kinetic model.

Table 6. Kinetic parameters (rate law, standard deviation taken from linear regression, R^2 values and half-life) for zero-order, first-order and pseudo second-order models for the iodine released into the 1 M Na-dithionite + 0.4 M K_2CO_3 solution in samples E84-86

Sample ID	Borehole	Zero-order		First-order		Pseudo second-order	
		k (\pm StDev) ($\mu\text{g/L}\cdot\text{h}^{-1}$)	R^2	k (\pm StDev) (1/h)	R^2	k (\pm StDev) [1/[($\mu\text{g/L}$) \cdot h]]	R^2
E84	C9507 104.4-105.4'	1.336 \pm 0.300	0.798	0.0146 \pm 0.0041	0.386	0.0042 \pm 0.0002	0.984
E85	C9510 114.3-115.3'	0.835 \pm 0.206	0.768	0.0103 \pm 0.0036	0.482	0.0061 \pm 0.0003	0.989
E86	C9507 94.1- 95.1'	0.0345 \pm 0.0195	0.385	0.0411 \pm 0.0128	0.493	0.1009 \pm 0.0042	0.993

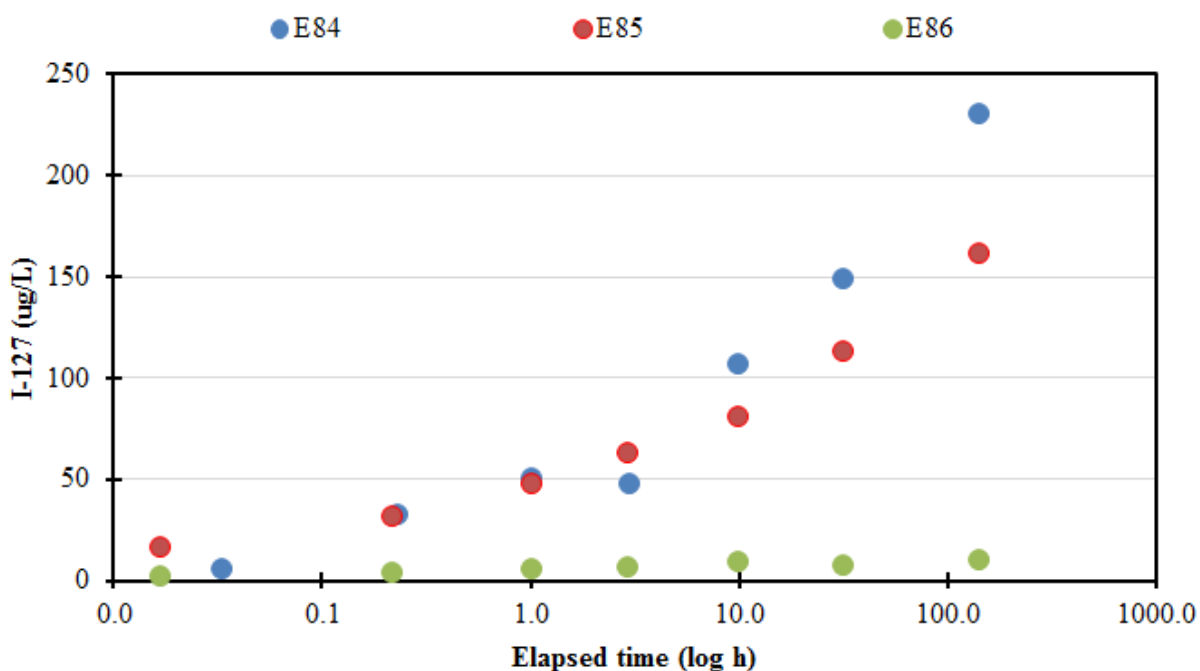


Figure 6. Iodine-127 extracted from soil sediments sample E84 - borehole C9507 104.4-105.4' (blue), sample E85 - borehole C9510 114.3.115.3' (red), and sample E86 borehole - C9507 94.1-95.1' by 1 M Na-dithionite + 0.4 M K_2CO_3 in artificial groundwater solution as a function of time expressed in log hours.

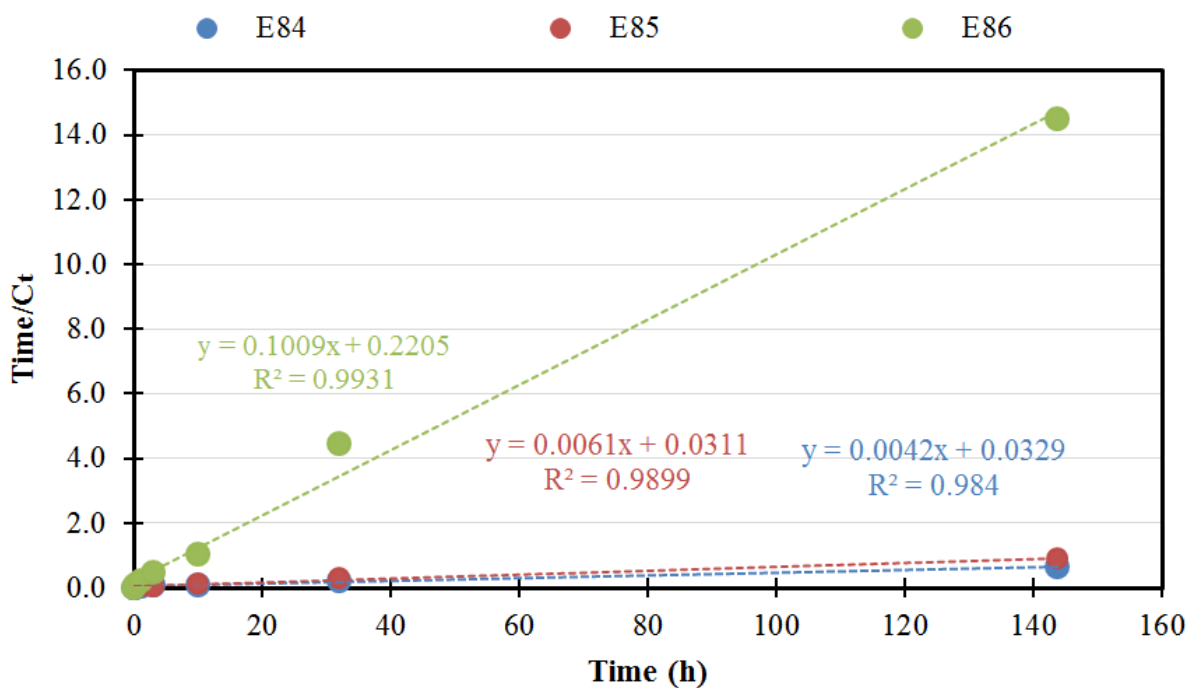


Figure 7. Pseudo second-order kinetics fit for iodate-contaminated (~100 µg/L) Hanford Site sediments; sample E84 (blue), sample E85 (red), and sample E86 (green).

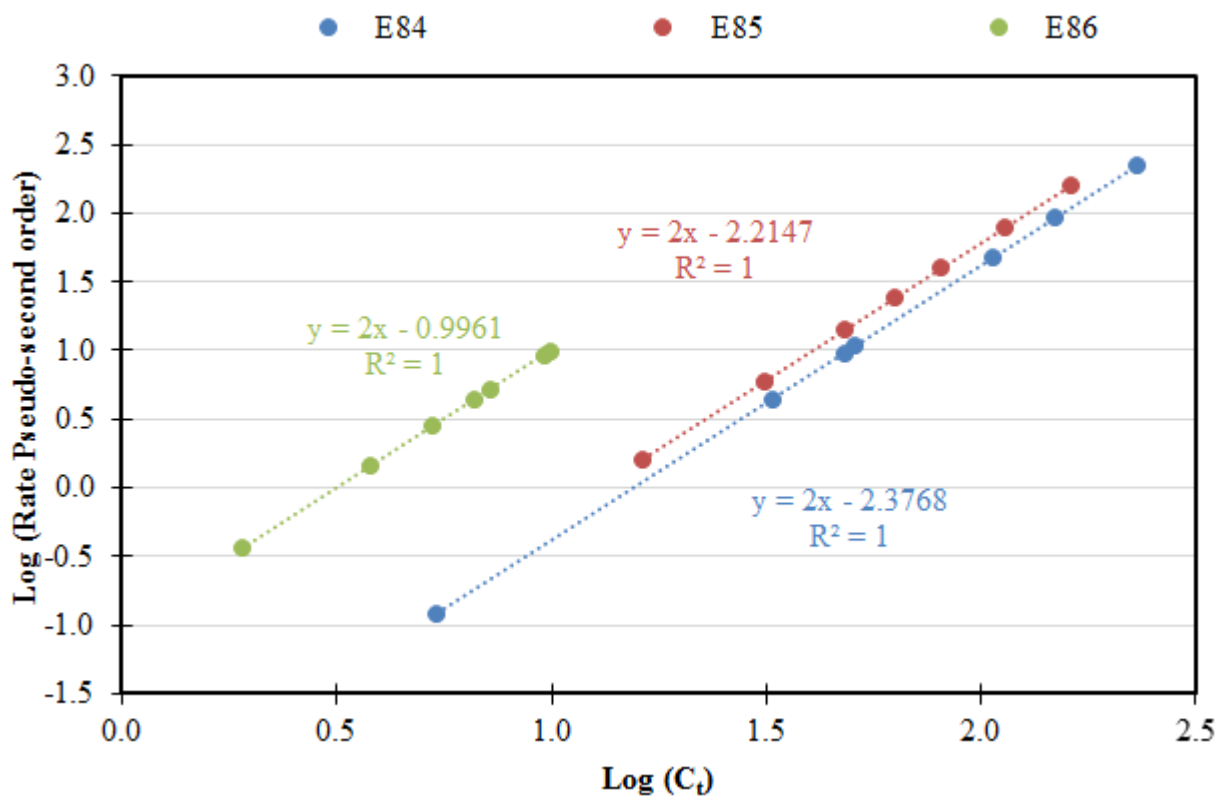


Figure 8. Reaction order plot of natural logarithm for the pseudo second-order rate using Eq. 5 against the natural logarithm of iodide concentration (in µg/L) for iodate-contaminated (~100 µg/L) Hanford Site sediments; sample E84 (blue), sample E85 (red), and sample E86 (green).

Part C. Long Term Stability of Iodine Leaching from Sediment - Batch System

Iodine analysis for the long-term stability is waiting to be analyzed by the Energy Systems Laboratory (EML). Therefore, these data will not be presented in this report.

5. CONCLUSION

^{129}I is present in several large, though dilute, plumes in the groundwater at the DOE Hanford Site. ^{129}I is an uncommon contaminant and remediation technologies are limited for this highly mobile anion. At the Savannah River Site (SRS) sediments are greatly weathered and rarely contain carbonate phases with a groundwater pH between 3.1 and 5, iodine is less mobile. However, at the Hanford Site subsurface sediments contain young minerals and large amounts (~2%) of carbonate minerals, with a higher pH value of 7 to 8.5. Because of these alkaline, nonreducing environmental conditions, the abundance of iodate is maintained (Strickland et al., 2017; Zhang et al., 2013) although there is the potential for incorporation of iodine in carbonate and Fe oxide precipitates.

In this study, batch experiments were conducted to quantify iodine dissolution into the aqueous phase via Na-dithionite treatment as a potential remediation technology. Experiments were divided into three parts (Parts A-C) to target two specific aims. For Part C, analysis is still being conducted. For Part A, contaminated sediment from borehole C9510 114.3-115.3 in OU 200-UP-1 was exposed to variable solution components. Results show that 48-hr contact time of Na-dithionite and carbonate buffer solution, K_2CO_3 (sample E83), was the most effective on iodine leaching in comparison to non-freshly added reductant solution sediments (samples E80-82) that underwent a seven-day contact time.

For Part B experiments, ^{127}I leaching was plotted as a function of contact time (Figure 6). For all three samples (sample ID E84-86), iodide leaching was still increasing (i.e., unreached steady-state). For all three samples, sample ID E84 (borehole C9507 104.4-105.4') showed the most mobilization. Sample ID E84 leached 230 $\mu\text{g/L}$ of iodide in comparison to sample ID E86 (borehole C9507 94.1-95.1') that leached 9.9 $\mu\text{g/L}$. In addition, both Parts A and B experiments support previous studies that the combination of 0.1 M Na-dithionite with K_2CO_3 buffer solution was the most effective in the mobilization of iodine species (Boparai et al., 2008; Cervini-Silva et al., 2001; Szecsody et al., 2004; Zachara et al., 2000).

When trying to fit Part B dataset into a kinetic model, the overall reaction was found to be pseudo second-order with respect to the dithionite concentration. Assuming pseudo second-order dependence with respect to iodide, the rate law constant was calculated as $0.004 \pm 0.000 \mu\text{g} / \text{L}^{-1} \cdot \text{h}^{-1}$, $0.0061 \pm 0.000 \mu\text{g} / \text{L}^{-1} \cdot \text{h}^{-1}$, and $0.101 \pm 0.004 \mu\text{g} / \text{L}^{-1} \cdot \text{h}^{-1}$ for samples E84, E85 and E86, respectively. In addition, when using the method of initial rates to determine the reaction order, a plot of the natural logarithm for the pseudo second-order rate against the natural logarithm of iodide concentration (in $\mu\text{g/L}$) (Figure 8) yielded a power of two, indicative of a pseudo second-order reaction kinetic fit.

Although further experiments are required to fully understand the Na-dithionite system and parameters controlling leaching rates, preliminary conclusions can be drawn based on the data gathered during this internship. The reductant Na-dithionite promises to be a potential technology to mobilize the uncommon contaminant ^{129}I at the DOE's Hanford Site.

6. REFERENCES

- Atkins, P., & DePaula, J. (2010). *Physical Chemistry* (9th ed.). Oxford: Oxford.
- Boparai, H. K., Comfort, S., Shea, P. J., & Szecsody, J. E. J. C. (2008). Remediating explosive-contaminated groundwater by in situ redox manipulation (ISRM) of aquifer sediments. *Chemosphere*, 71(5), 933-941.
- Cervini-Silva, J., Larson, R. A., Wu, J., Stucki, J. W. J. E. s., & technology. (2001). Transformation of chlorinated aliphatic compounds by ferruginous smectite. 35(4), 805-809.
- Devlin, J., & Müller, D. (1999). Field and laboratory studies of carbon tetrachloride transformation in a sandy aquifer under sulfate reducing conditions. *Environmental Science & Technology*, 33(7), 1021-1027.
- Kantelo, M., Bauer, L., Marter, W., Murphy Jr, C., & Zeigler, C. (1993). Radioiodine in the Savannah River site environment: Westinghouse Savannah River Co., Aiken, SC (United States).
- Kaplan, D. I., Denham, M. E., Zhang, S., Yeager, C., Xu, C., Schwehr, K., . . . technology. (2014). Radioiodine biogeochemistry and prevalence in groundwater. 44(20), 2287-2335.
- Strickland, C. E., Johnson, C. D., Lee, B. D., Qafoku, N., Szecsody, J. E., Truex, M. J., & Vermeul, V. R. (2017). Identification of promising remediation technologies for iodine in the UP-1 Operable Unit: Pacific Northwest National Lab.(PNNL), Richland, WA (United States).
- Stucki, J. W., Golden, D., Roth, C. B. J. C., & Minerals, C. (1984). Preparation and handling of dithionite-reduced smectite suspensions. 32(3), 191-197.
- Szecsody, J. E., Fruchter, J. S., Williams, M. D., Vermeul, V. R., Sklarew, D. J. E. s., & technology. (2004). In situ chemical reduction of aquifer sediments: Enhancement of reactive iron phases and TCE dechlorination. 38(17), 4656-4663.
- Szecsody, J. E., Lee, B. D., Lawter, A. R., Qafoku, N., Resch, C. T., Baum, S. R., . . . Freedman, V. L. (2017). Effect of Co-Contaminants Uranium and Nitrate on Iodine Remediation: Pacific Northwest National Lab.(PNNL), Richland, WA (United States).
- Waybrant, K., Blowes, D., & Ptacek, C. (1998). Selection of reactive mixtures for use in permeable reactive walls for treatment of mine drainage. *Environmental Science & Technology*, 32(13), 1972-1979.
- Zachara, J. M., Foster, N. S., Amonette, J. E., Bylaska, E. J., Felmy, A. R., Gassman, P. L., . . . Mason, M. J. (2000). Annual Report 1999 Environmental Dynamics & Simulation: Pacific Northwest National Lab.(PNNL), Richland, WA (United States).
- Zhang, S., Xu, C., Creeley, D., Ho, Y.-F., Li, H.-P., Grandbois, R., . . . technology. (2013). Iodine-129 and iodine-127 speciation in groundwater at the Hanford Site, US: Iodate incorporation into calcite. 47(17), 9635-9642.

APPENDIX A.

Additional PNNL Internship activities and DOE-sponsored tours

As part of the Alternative Sponsored Fellow internship program at PNNL, interns have the chance to participate in tours. One particular tour consists of visiting the world's first nuclear production B-reactor "Manhattan Project" at Hanford's 200 Area (Figures 9 and 10). This was a wonderful opportunity not only to admire the magnitude of the reactor's engineering, but also to understand how and why this research is appropriate and useful to the Hanford Site. In addition, interns were able to explore the Environmental Molecular Sciences Laboratory (EMSL), PNNL's DOE scientific user facility (Figure 11), the 3D printing room mostly used to build batteries (Figure 12) and the Aquatic Research Laboratory (ARL) where many species of cold- and warm-water fishes are grown and studied (Figure 13). Further, Figure 14 shows Di Pietro with MSIPP fellow Jonathan Williams in front of one of the two infrared detector arms at the Laser Interferometer Gravitational-Wave Observatory (LIGO) tour, where gravitational waves were detected in September of 2015. Figures 15-17 show the field site of polyphosphate injection to remediate uranium in the 300 Area (0.5 mi N of building 331). Di Pietro also participated in a five-hour guided tour of the Hanford Clean Up Sites. In this tour, reactors KE, KW, N, DR and D, B and T plant were shown. In addition, the 200 West and East Ares were explained and visited from the bus. Lastly, a detailed tour was given on the Vitrification plant, the largest construction site currently being undertaken in the US. For this tour, no photos were allowed.

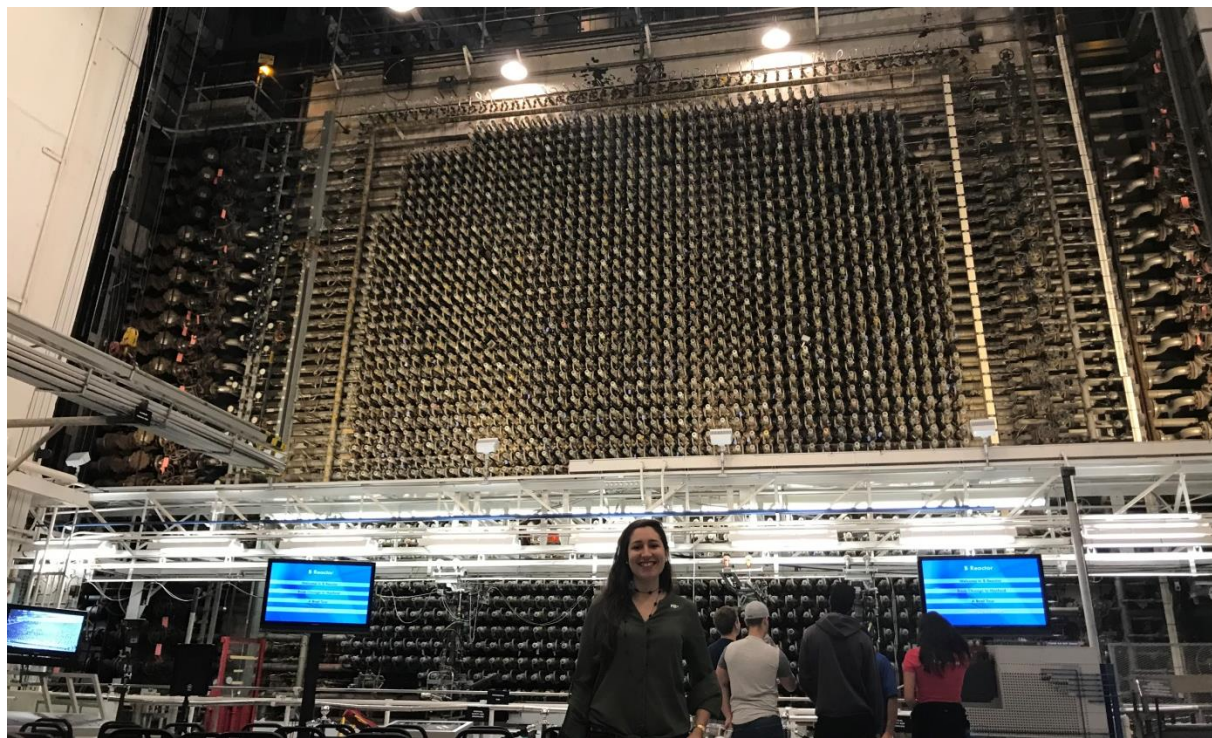


Figure 9. National Historic Landmark Nuclear Production Plant B-reactor constructed in 1943-1944.



Figure 10. DOE Fellow Silvina Di Pietro in front of the B-Reactor National Historic Landmark entrance.

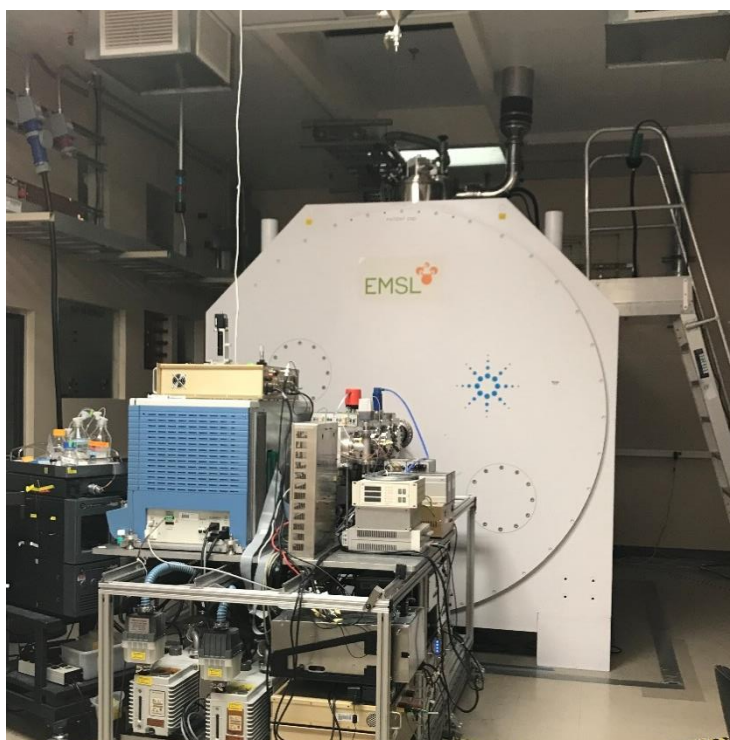


Figure 11. Nuclear Magnetic Resonance (NMR) coupled with Ion Cyclotron Resonance (ICR) instrument with 21.1 Tesla fields (900 MHz ^1H frequency) from EMSL facility.

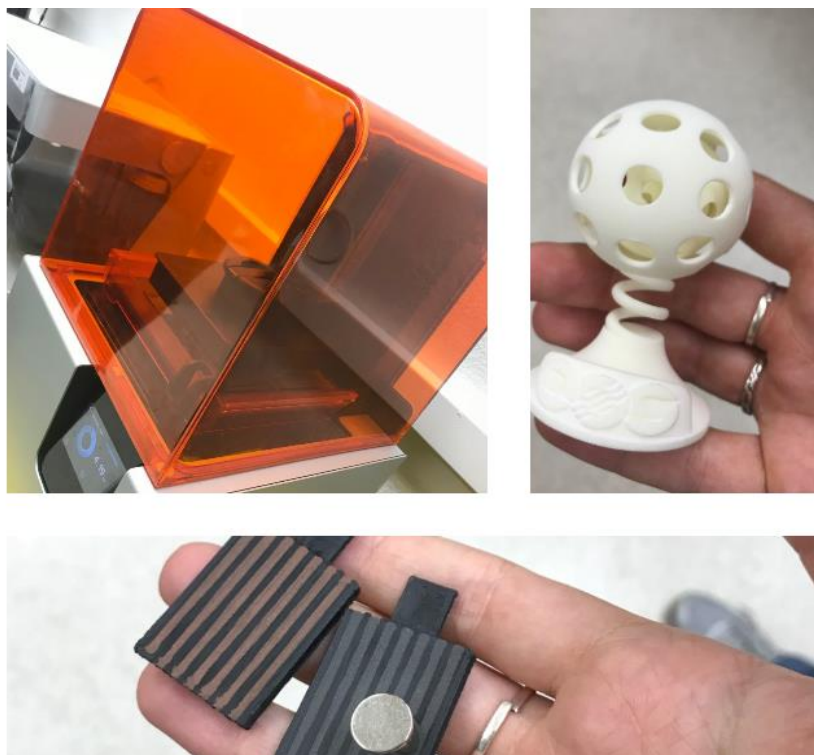


Figure 12. 3-D printing facility showing batteries and spherical balls Matryoshka-design as samples.



Figure 13. Tanks in the Aquatic Research Laboratory; guided tour by P.I. Timothy Linley.



Figure 14. Jonathan Williams, MSIPP fellow and FIU biomedical engineering student, with DOE Fellow Silvina Di Pietro in front of one of the two detector arms of the Laser Interferometer Gravitational-Wave Observatory (LIGO) at Hanford, WA.



Figure 15. FF-5 Stage B polyphosphate tanks in the 300 Area treatment field.



Figure 16. One of the 48 wells (painted yellow) dug into the subsurface of the FF-5 Stage B, 300 Area treatment field (Columbia River pictured at the right).



Figure 17. Contractors (right) show PNNL scientists (left) how the pump delivers the polyphosphate solution to the wells.